W-boson-plus-two-jet production at the Fermilab Tevatron

Michelangelo Mangano
Istituto Nazionale di Fisica Nucleare, San Piero a Grado, Pisa, Italy

Stephen Parke
Fermi National Accelerator Laboratory, P.O. Box 500, Batavia, Illinois 60510
(Received 3 August 1989)

In this paper we present a detailed study of rates and distributions for the production of a W boson plus two jets at the Fermilab 1.8-TeV Collider, assuming that the top quark does not contribute to these events. This process is the principal background to the discovery of a top quark in the 80–110-GeV range with 5 pb^{-1} of data at the Fermilab Tevatron.

I. INTRODUCTION

In proton-antiproton colliders, the processes which give rise to events with a W boson and jets are of great interest for the discovery of a top quark with mass near or above the mass of the W boson. For such a heavy top quark the dominant production mechanism results in the production of both a top quark and a top antiquark:[1]

$$p + \bar{p} \rightarrow t + \bar{t} + X \ .$$

Both of these top quarks decay into a W boson (real or virtual) plus a b quark. Subsequently, the two W's decay either leptonically or hadronically. However, if both W bosons decay leptonically the signal rate is very small, while if both W's decay hadronically the signal rate is swamped by QCD jet processes. If one of the W's decays leptonically and the other hadronically the signal consists of a "leptonic W" (charged lepton plus missing P_T) plus jets. Unfortunately, there is a background to this type of event from non-top processes in the standard model.

For a top-quark mass just above the W-boson-plus-b-quark mass threshold, the b quarks produced by the decay of either top quark will not be observed in the detector most of the time because of their small transverse momentum. Therefore, near this threshold, with one W boson decaying leptonically and the other hadronically, the signal will be predominantly a "leptonic W" plus two jets. For a higher-mass top quark the W boson plus three- or four-jet signal will become more important. The matrix elements for the W plus three-jet processes have been calculated recently.[2]

The Collider Detector at Fermilab (CDF) has collected approximately 5 pb^{-1} of data at $\sqrt{s} = 1.8$ TeV at the Tevatron. With this quantity of data, the top signal from both W's decaying leptonically runs out of events for a top-quark mass around the mass of the W or Z bosons. To extend the discovery range for the top quark at CDF with the present amount of data one must turn to the W-boson-plus-jets signal. In this paper we present a detailed study of various differential distributions for the W-boson-plus-two-jet background to the detection of the top quark. In particular, we emphasize the Q^2 dependence of both rates and distributions. Given the uncertainty in the absolute rates due the different possible choices of Q^2, it becomes important to establish whether this has an impact on the *shapes* of the distributions as well.

The following section describes the calculation while Sec. III contains the results of this calculation followed by the conclusions. Many papers have appeared recently which study top signals at hadronic colliders and production rates for relevant backgrounds: in Ref. 3 we present a (possibly incomplete) list.

II. THE CALCULATION

The W-boson-plus-two-jet cross section at the Tevatron is dominated by the processes involving $q\bar{q}ggW$ (Ref. 4). The amplitude for these processes with the subsequent decay of the W boson has been calculated to lowest order in perturbation theory in Refs. 5, 6, and 7. We have independently recalculated the relevant matrix elements, and have checked numerically against previous calculations (taking into account all the spin correlations between the final-state leptons and the quarks). For proton antiproton collisions the W boson plus two jet events have contributions from the quark-antiquark, quark-gluon, antiquark-gluon, and two-gluon initial states. As in any tree-level QCD processes these amplitudes are singular in the limits when two partons are collinear or when one parton is soft. To control these singularities we have made cuts on the allowed phase space of the partons. Of course the experimental definition of jets also requires the introduction of isolation and minimum-energy cuts; therefore, we have used realistic criteria to constrain the phase space of the final-state

partons. Two different sets of cuts have been used for the jets corresponding to a high and a low jet-transverse-momentum P_T threshold. The jet cuts are

$$P_T > 22 \text{ GeV or } P_T > 15 \text{ GeV},$$
$$|\eta| < 2, \tag{2.1}$$
$$\Delta R_{JJ} \equiv \sqrt{\delta\eta^2 + \delta\phi^2} > 0.7,$$

where η is the pseudorapidity of the jets and ϕ is the azimuthal angle around the beam direction. When taking into account the effects of energy loss outside the jet cone because of fragmentation and the reduced low-energy response of the calorimetry, the high and low P_T thresholds for the partons roughly correspond to a measured P_T of the jets of approximately 15 and 10 GeV, respectively.

In this calculation we only include the contribution from the electron-decay of the W boson, but the other leptonic decays can be included by a trivial multiplicative factor. For the electron and neutrino the P_T cut used is

$$P_T > 20 \text{ GeV} \tag{2.2}$$

and the electron is required to be in the central region but isolated from the jets, these last cuts being

$$|\eta| < 1, \quad \Delta R_{eJ} > 0.4. \tag{2.3}$$

In the Appendix we give the cuts and the total cross section for the analogous calculation involving a Z boson; i.e., proton plus antiproton goes to Z boson plus two jets where the Z boson decays into an electron-plus-positron pair.

We have used the Eichten-Hinchliffe-Lane-Quigg (ELHQ) 1 structure functions with $\Lambda_{\rm QCD} = 200$ MeV. Since we expect the cross section to be sensitive to the choice of Q^2, we have used a variety of possible values for Q^2. Some of these choices depend on the kinematics of the event while others are kinematically neutral. This sensitivity to the choice of Q^2 could be reduced if the next-to-leading-order contributions to the cross section were available.

III. THE RESULTS

The results of the calculation described in the previous section are summarized in the tables and figures in this section. Using the cuts for the partons and leptons described by Eqs. (2.1)–(2.3) the total cross section has been calculated for the following choices of Q^2: (1) the transverse energy squared of the W boson, $M_W^2 + (P_T)_W^2$, (2) the mass squared of the dijet system, M_{JJ}^2, (3) the square of the arithmetic mean of the P_T of the jets, $(\sum P_T/2)^2$, and (4) the mass squared of the W boson, M_W^2.

The magnitudes of the total cross sections for these values of Q^2 are summarized in Table I.

As expected there is quite a range of values for the total cross section depending on the choice of Q^2. The percentage change in the total cross section is larger for the lower jet-P_T threshold than for the higher threshold. This is easily understood because for the higher P_T threshold the difference between the various choices of Q^2 is not as large as for the lower P_T threshold.

TABLE I. Rates for W-plus-two-jet production (Q^2 dependence).

Q^2	Jet P_T >22 GeV (pb)	Jet P_T >15 GeV (pb)
$M_W^2 + (P_T)_W^2$	7.8	17
M_{JJ}^2	8.6	21
$\left(\sum P_T^j/2\right)^2$	11	27
M_W^2	8.5	18

If one were to vary the kinematically neutral $Q^2 = M_W^2$ by multiplying or dividing this Q^2 by some factor the shapes of the above curves would remain unchanged yet their normalizations would be different. However the other choices of Q^2 are not kinematically neutral and tend to increase that part of the cross section which contains softer jets. This can be seen by comparing the M_W^2 cross section with that obtained using M_{JJ}^2, in Table I. The high-P_T threshold cross section varies little for this change of Q^2 whereas the low-P_T threshold cross section is increased by 20%. Similar comparisons can be made between the other choices of Q^2.

In Table II we compare the production rates calculated using different choices of structure functions,[8] namely Duke-Owens (DO) sets 1 and 2, EHLQ set 1, and Glück-Hoffman-Reya (GHR). We fixed $Q^2 = M_W^2 + (P_T)_W^2$.

The shape of the cross section is described by the following figures, in which we compare differential distributions obtained using the first three choices of Q^2 listed above. We have plotted the following differential cross sections: $d\sigma/dP_T$ for the jet P_T, electron P_T and the W-boson P_T, in Figs. 1–3. Figure 4 is the differential cross section with respect to the dijet mass of the jets and Fig. 5 is the differential cross section with respect to the sum of the scalar E_T of the jets. Figures 6 and 7 are the differential cross sections with respect to the azimuthal angle of the two leptons and two jets, respectively, whereas Fig. 8 is the differential cross section with respect to the difference in pseudorapidity of the two jets. Figure 9, finally, contains the transverse-mass distribution of the electron-neutrino pair.

TABLE II. Rates for W-plus-two-jet production (structure-function dependence).

Structure function	Jet P_T >22 GeV (pb)	Jet P_T >15 GeV (pb)
DO 1	8.3	18
DO 2	9.4	22
EHLQ 1	7.8	17
GHR	11	23

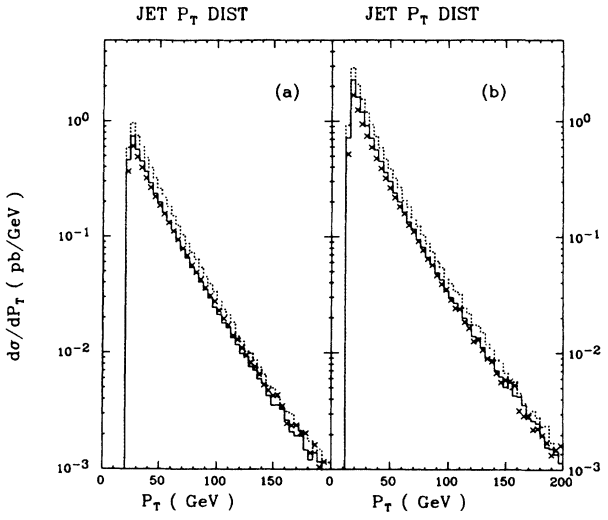

FIG. 1. The differential cross section $d\sigma/dP_T$ versus jet P_T. Both partons in each event enter in the histogram. The solid line corresponds to $Q^2 = M_{JJ}^2$, the dotted line to $Q^2 = (\sum P_T^j/2)^2$ and the points correspond to $Q^2 = M_W^2 + (P_T)_W^2$. Part (a) corresponds to the high-P_T jet threshold, (b) to the low-P_T jet threshold.

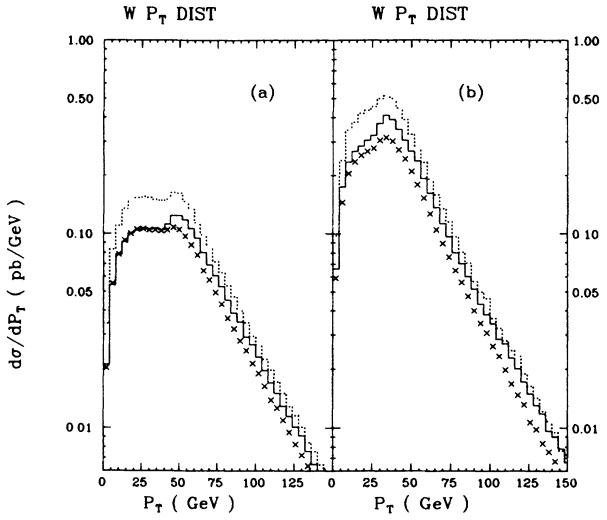

FIG. 3. The differential cross section $d\sigma/dP_T$ versus P_T of the W boson. Symbols and notations as in Fig. 1.

As can be seen, for some of the distributions a change in Q^2 amounts not just to a change in rate, but to a change of shape as well, and this has to be kept in mind when comparing data with theory.

Figure 4 is particularly useful for the search for the top quark since for top-induced W-boson-plus-two-jet events the two jets are expected to come from the hadronic decay of a W boson. Therefore their invariant mass is expected to be the mass of the W boson up to detector mass resolution. Choosing $Q^2 = M_W^2$ the cross section for the background with the two jets having a mass within 15 GeV of the mass of the W boson is 4.5 and 2.7 pb for the low- and high-P_T thresholds, respectively. From Fig. 7, the differential cross section with respect to the azimuthal angle of the two jets demonstrates that the jets are predominantly formed back to back and that the ΔR cut for the jets successfully cuts off the collinear singularity as the two jets become parallel.

In order to briefly study the possible effects of the detector-energy corrections on the measured quantities, we also recalculated the distribution of the azimuthal difference between the leptons by using the direction of the

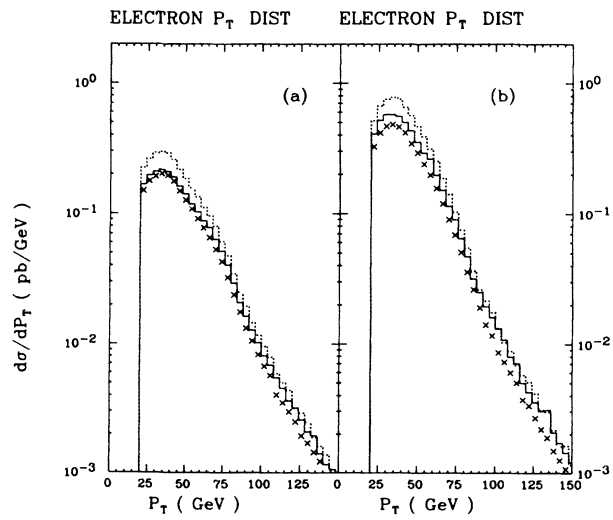

FIG. 2. The differential cross section $d\sigma/dP_T$ versus P_T of the electron. Symbols and notations as in Fig. 1.

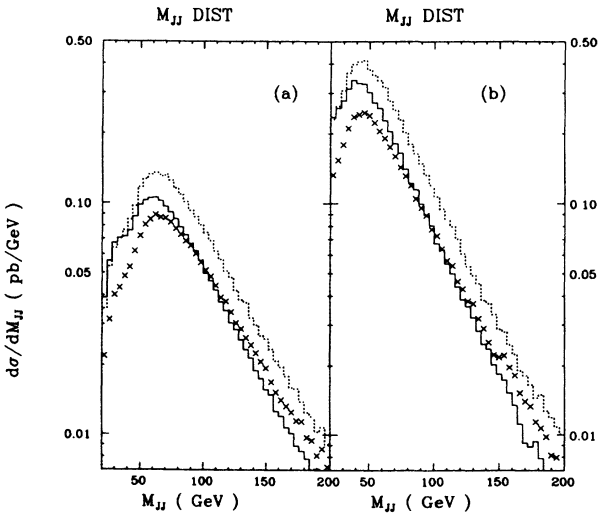

FIG. 4. The differential cross section $d\sigma/dM_{JJ}$ versus the dijet mass, M_{JJ}, of the jets. Symbols and notations as in Fig. 1.

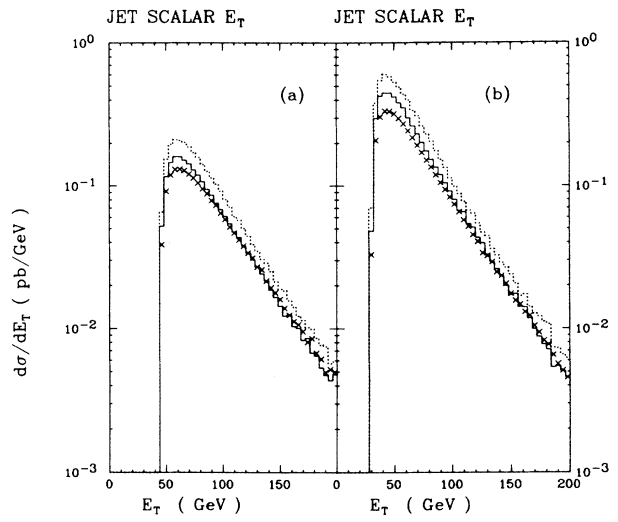

FIG. 5. The differential cross section $d\sigma/dE_T$ versus the scalar E_T sum of the jets. Symbols and notations as in Fig. 1.

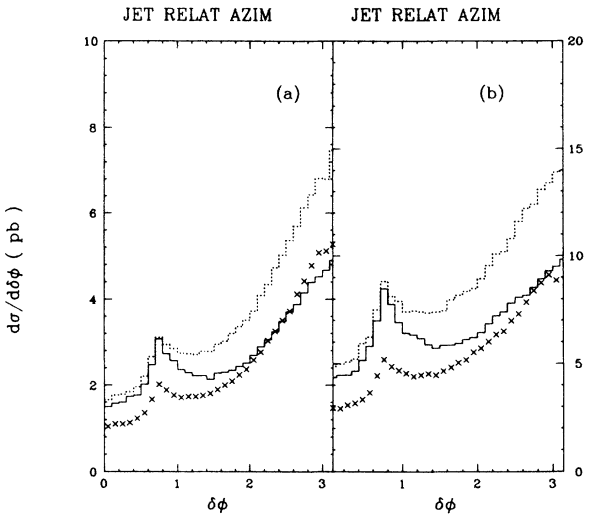

FIG. 7. The differential cross section $d\sigma/d\phi_{JJ}$ versus the azimuthal angle ϕ_{JJ} of the jets. Symbols and notations as in Fig. 1.

raw missing energy rather than the *true* energy of the neutrino. The raw missing energy is defined as the norm of the vector sum of the transverse momentum of the electron plus the raw transverse momenta of the jets, given by

$$E_T = 1.2\, E_T^{\rm raw} + 3\,, \tag{3.1}$$

where this relation can be used as a "rule of thumb" conversion between the parton energy and the energy of the observed jet resulting from the evolution of the parton itself. Choosing $Q^2 = M_{JJ}^2$ we show in Fig. 10 the relative azimuthal distribution of the leptons as compared to the relative azimuthal distribution of electron and raw missing E_T, to emphasize with an example the fact well known to experimentalists that jet energy corrections may in fact change not just scale factors, but shapes as well. Of course the energy resolution effects will further smear the curve shown in Fig. 10.

IV. CONCLUSIONS

In this paper we have given details on the shape and normalization to the W-boson-plus-two-jet cross section

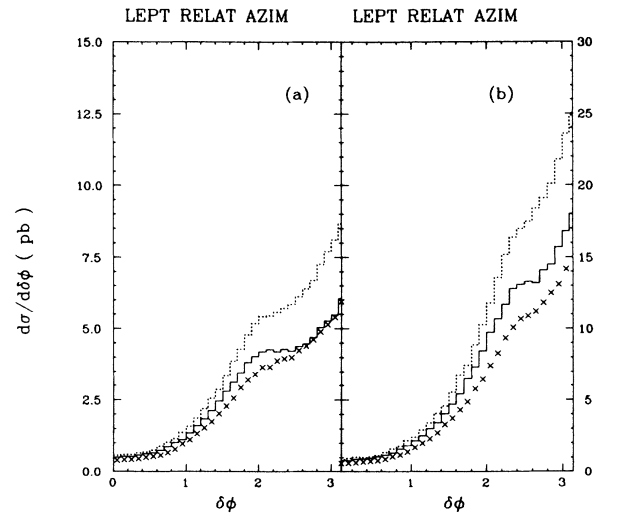

FIG. 6. The differential cross section $d\sigma/d\phi_{l\bar{l}}$ versus the azimuthal angle $\phi_{l\bar{l}}$ of the leptons. Symbols and notations as in Fig. 1.

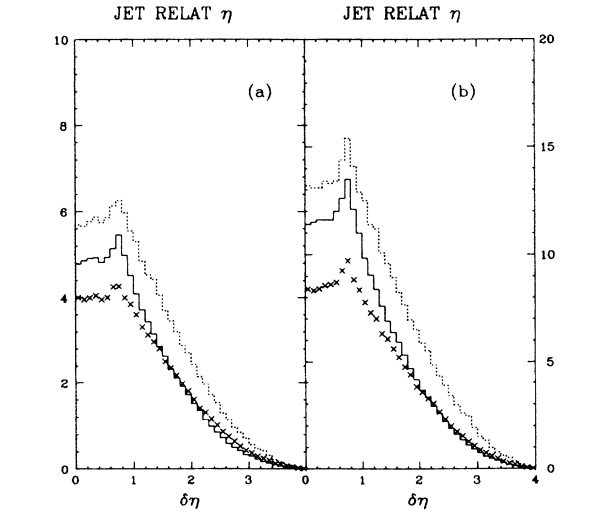

FIG. 8. The differential cross section $d\sigma/d\eta_{JJ}$ versus the difference in the pseudorapidity, η_{JJ}, of the jets. Symbols and notations as in Fig. 1.

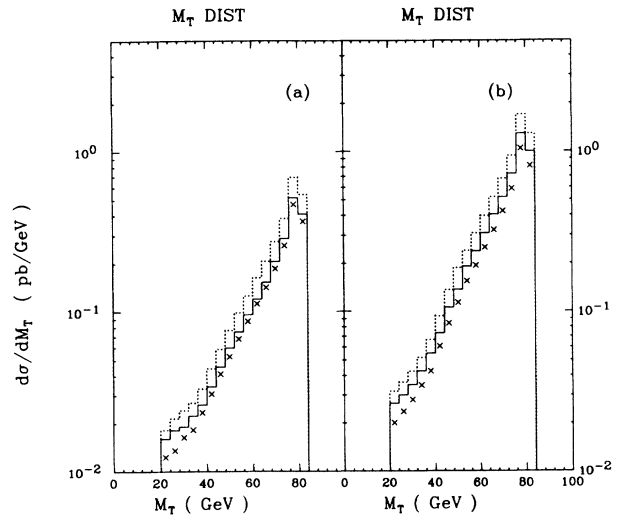

FIG. 9. The differential cross section $d\sigma/dM_T$ versus the W transverse mass, defined by $M_T^2 = 2P_T^e P_T^\nu(1-\cos\phi)$. Symbols and notations as in Fig. 1.

for proton-antiproton collisions at 1.8 TeV in the center of mass. The W boson is assumed to be observed in the electron-neutrino decay mode. This process is the dominant background to the discovery of the top quark with a mass between 80 and 110 GeV at CDF with 5 pb^{-1} of data. Since these background cross sections are of the order of 10 pb (20 pb) for the high (low) jet-P_T threshold, there should be at least 50 (100) events of this type in the current data set. This number of events should allow

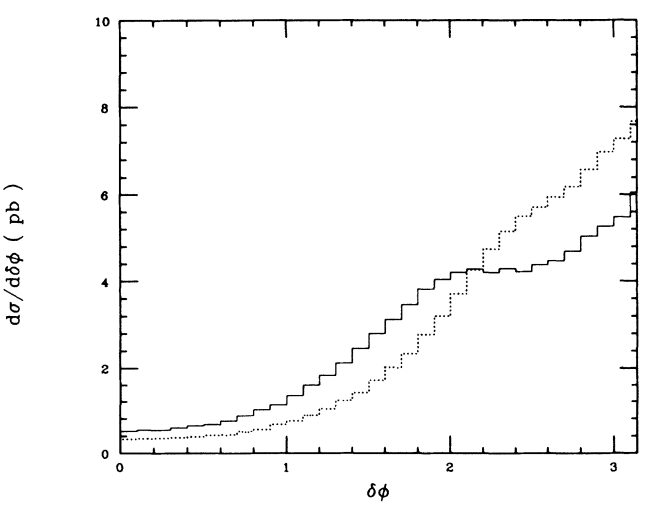

FIG. 10. The differential cross section $d\sigma/d\phi$ versus the relative azimuth between electron and neutrino (solid line) and between electron and raw missing E_T (dotted line). We used $Q^2 = M_{JJ}^2$ and the high-P_T jet threshold.

TABLE III. Cross sections for Z-plus-two-jet production at the Fermilab Tevatron.

Q^2	Jet P_T >22 GeV (pb)	Jet P_T >15 GeV (pb)
$M_Z^2 + (P_T)_Z^2$	1.5	3.2
M_{JJ}^2	1.7	4.1
$\left(\sum P_T/2\right)^2$	2.2	5.2

a reasonable comparison between theory and experiment not only on the total rate but also on shape of the cross section. Hopefully discrepancies will be found which may indicate the presence of an additional signal, e.g., the top quark.

ACKNOWLEDGMENTS

We are thankful to J. Yoh and G.P. Yeh for many useful discussions and suggestions related to this work. Fermilab is operated by the Universities Research Association Inc. under contract with the United States Department of Energy.

APPENDIX

For the Z-boson-plus-two-jet cross section we have again used cuts which closely mimic a realistic detector's cuts. Two different sets of cuts have been used for the jets corresponding to a high and a low jet-transverse-momentum P_T threshold. The jet cuts are

$$P_T > 22 \text{ GeV or } P_T > 15 \text{ GeV} ,$$

$$|\eta| < 2 , \tag{A1}$$

$$\Delta R_{JJ} \equiv \sqrt{\delta\eta^2 + \delta\phi^2} > 0.7 .$$

The high and low P_T thresholds for the partons roughly correspond to a measured P_T of the jets of 15 and 10 GeV, respectively. The only contribution included here is the decay of the Z boson into an electron-and-positron pair. The cuts imposed on these charged leptons are such that one must satisfy

$$P_T > 20 \text{ GeV} , \quad |\eta| < 1 , \tag{A2}$$

and the other is unbiased both in P_T and η. Both charged leptons are isolated from the jets by

$$\Delta R_{eJ} > 0.4. \tag{A3}$$

In Table III we present the results for the total cross section for the high and low P_T threshold for a number of choices of Q^2.

[1]P. Nason, S. Dawson and R. K. Ellis, Nucl. Phys. **B303**, 607 (1988); G. Altarelli, M. Diemoz, G. Martinelli, and P. Nason, *ibid.* **B308**, 724 (1988).

[2]K. Hagiwara and D. Zeppenfeld, Nucl. Phys. **B313**, 560 (1989); F. A. Berends, W. T. Giele, and H. Kuijf, *ibid.* **B321**, 39 (1989); F. A. Berends, W. T. Giele, H. Kuijf, R. Kleiss, and W. J. Stirling, Phys. Lett. B **224**, 237 (1989); V. Barger, T. Han, J. Ohnemus, and D. Zeppenfeld, Phys. Rev. D **40**, 2888 (1989).

[3]H. Baer, V. Barger, H. Goldberg, and R. J. N. Phillips, Phys. Rev. D **37**, 3152 (1988); R. Kleiss, A. D. Martin, and W. J. Stirling, Z. Phys. C **39**, 393 (1988); S. Gupta and D. P. Roy, *ibid.* **39**, 417 (1988); F. Halzen, C. S. Kim, and A. D. Martin, Mod. Phys. Lett. A **4**, 1531 (1989); H. Baer, V. Barger, and R. J. N. Phillips, Phys. Rev. D **39**, 3310 (1989); Phys. Lett. B **221**, 398 (1989); J. L. Rosner, Phys. Rev. D **39**, 3297 (1989).

[4]The processes involving $q\bar{q}q\bar{q}W$ have not been included because they contribute only 10% to the total cross section, which is much less than the uncertainty introduced by the sensitivity to the choice of Q^2. By neglecting these processes we have been able to perform higher statistics runs for a larger range of Q^2 values.

[5]J. Gunion and Z. Kunszt, Phys. Lett. **161B**, 333 (1985).

[6]R. Kleiss and W. J. Stirling, Nucl. Phys. **B262**, 235 (1985).

[7]R.K. Ellis and R.J. Gonsalvez, in *Supercollider Physics*, proceedings of the Oregon Workshop, Eugene, Oregon, 1985, edited by D. Soper (World Scientific, Singapore, 1987), p. 287; P. B. Arnold and M. H. Reno, Nucl. Phys. **B319**, 37 (1989).

[8]D. W. Duke and J. F. Owens, Phys. Rev. D **27**, 508 (1984); E. Eichten, I. Hinchliffe, K. Lane, and C. Quigg, Rev. Mod. Phys. **56**, 579 (1984); M. Glück, E. Hoffman, and E. Reya, Z. Phys. C **13**, 119 (1982).